5.6 Overmixing in Inverse Estuaries.

Ideas about overmixing and maximal flow have also been applied to inverse estuaries, most notably the Mediterranean and Red Seas. The overturning circulation and exchange flow is driven primarily by excessive evaporation that exists in the arid climates of these marginal seas. Historical estimates of *E-P* range from 0.5 to 1.0 *m/year* in the Mediterranean and roughly twice that amount in the Red Sea. The contribution Q_R^* from river runoff is minor in both cases and can be neglected in Knudsen's relations (5.5.3a,b). Evaporation concentrates salt in the surface waters, thereby increasing its density and leading to sinking. In some cases the evaporation preconditions the water for deep convection in response to atmospheric cooling events that take place in winter. In the two-layer idealization, upper layer water is mixed down into the lower layer and the exchange flow at the mouth, in this case the Strait of Gibraltar or the Bab al Mandab, is reversed relative to a normal estuary. The upper layer salinity S_1 at the mouth is considered to be the observable since it is this water that is drawn in from the outside ocean.

It should be kept in mind that the intensity of the mixing and deep convection in an inverse estuary is, in principle, a function of the *E-P* and/or the surface thermal forcing. It is therefore more difficult to think of mixing as an independent parameter in the way that estuary mixing might be considered independent of Q_R^*. Moreover, intensification of thermohaline forcing at the surface presumably causes the density of the product water to increase. That is, stronger forcing ostensibly leads to more mixing but also to an *increase* in the value of g'. In this situation it is unclear whether stronger surface forcing moves the system towards or away from an overmixed state.

In the Mediterranean and Red Seas, the exact sequence of events by which the outflow waters are produced and the geographical distribution of such events are not fully understood. In the Mediterranean, deep convection events have been observed in the Gulf of Lyon and the northern Aegean Sea. The Red Sea is not as well observed but it is known that the bulk of the outflow comes from an intermediate water mass that lies only 100-300 below the surface. In one view of the overturning circulation (Philips, 1969; see Exercise 1) the sinking occurs continuously over the whole area of the sea. Sporadic deep convection events in the northern reaches of the Red Sea (Woelk and Quadfasel, 1996) produce a deeper water mass that contributes a lesser amount to the outflow. The dynamics of the overturning circulation are further complicated during the summer monsoon by the appearance of a three-layer exchange flow in the Bab al Mandab.

The overmixing hypothesis was first applied to the Mediterranean Sea by Bryden and Stommel (1984). As in the original estuary formulation, the density difference between the two layers is due primarily to the salinity difference, and thus (5.5.5) continues to hold. The arguments leading to the Figure 5.5.1 curve can be repeated with river runoff Q_R^* replaced by $\iint_{A_s} (E - P)dA$ and S_1, rather than S_2, considered known.

The approach to the limit of overmixing occurs as a result of the descent along the left or

right branch of the curve until the maximal flux permitted by the mouth geometry is reached. For an estuary, this descent occurs as a result of holding Q_R^* fixed and supposing that S_2-S_1 decreases as a direct result of increased mixing. This scenario is more problematic for an inverse estuary where increased mixing due to increased $\iint_{A_s} (E-P)dA$ might actually *increase* S_2-S_1. Regardless of how it is achieved, the minimum possible salinity difference corresponding to the overmixed and maximal exchange conditions is found to be

$$(S_2 - S_1) = \left(\frac{\rho_2 S_1^2}{q_2^2 (D_s / z_T^*) g \beta w_m^{*2} D_s^{3}} \right)^{1/3} \left(\iint_{A_s} (E-P)dA \right)^{2/3}. \qquad (5.6.1)$$

As discussed in Sections 5.3 and 5.4, the coefficient $q_2(D_s/z_T^*)$ ranges between 0.208 and 0.25 as the geometry changes from a sill with infinitely deep upstream basin ($D_s/z_T^*=0$) to a pure contraction ($D_s/z_T^*=1$). It has been assumed that the sill lies at the point of minimum width in the mouth and that there is no barotropic flow.

Bryden and Stommel employ the pure contraction limit of (5.6.1) along with $E-P=0.95m/year$ to obtain $S_2-S_1=1.7\,°/_{oo}$, not far from the observed value $2.1\,°/_{oo}$. This estimate has been refined by later investigators who considered physically separated sill and narrows and weak barotropic inflow. In the case of Gibraltar, the shallowest sill lies adjacent to Camarinal (Figure 5.6.1) while the narrowest section lies at Tarifa. Through the work of Farmer and Armi (1986) it is now understood that maximal flow under these conditions tends to have one control at the narrows (where the upper layer is most active) and the other at the sill (where the lower layer is most active). Further refinements can be introduced through the use of non-rectangular cross-sections to more accurately represent the true topography (Bormans and Garrett 1989, and Dalziel 1991). The most refined model to date is due to Bryden and Kinder (1991), who also describe this history in more detail. Their predictions based on maximal exchange are $S_2-S_1=2.0\,°/_{oo}$, $Q_2^*=0.88\times10^6$ m^3/s, and $Q_1^*=-0.92\times10^6$ m^3/s as compared with contemporary observations $S_2-S_1=2.1$ $°/_{oo}$, $Q_2^*=(0.67\pm0.04)\times10^6$ m^3/s, and $Q_1^*=-(.78\pm0.17)\times10^6$ m^3/s (Tsimplis and Bryden, 2000).

Debate continues as to whether the Gibraltar exchange flow is maximal or slightly submaximal (Garrett 2004). Although a hydraulic jump is observed at the western end of the strait, it is less clear whether such a jump occurs at the eastern end. In addition, the flow is strongly modulated by the tides, which can cause the observed jump to break up and travel away as a train of internal waves. A comprehensive documentation of the flow over a tidal phase appears in Armi and Farmer (1989). Despite these complications, the reasonable agreement with observations has made the Mediterranean Sea/Gibraltar system the most promising large-scale application of the theory of overmixing.

In the Bab al Mandab, the exchange flow does not appear to be maximal. The sill and narrowest section occur at different locations and the flow at the latter appears to be

subcritical (Pratt, et al. 1999). The exchange flow therefore lacks the double critical section characteristics of maximal exchange. The Red Sea therefore does not appear to be overmixed, or even close to such a state, despite the fact that it is subject to fierce evaporation and winter cooling and that the sill depth is about the same as at Gibraltar. This apparent incongruity could be explained by the failure of one of the many assumptions leading to the hypothesis of overmixing. One of the most fundamental is that an increase in the sea surface forcing pushes the system towards maximal exchange. Intuitively, one would expect Q_2^* to increase as the rate of convection-generating buoyancy loss to the atmosphere is increased. However, the turbulence generated by vertical convection and the associated eddy stresses must also increase as the convection becomes more active. The resultant eddy momentum stresses may actually retard the exchange flows, making it difficult to predict how rapidly Q_2^* will actually increase. In summary, it is not obvious that an increase in E-P must cause the solution to *descend* along the Figure 5.5.1 solution curve (or its equivalent for an inverse estuary).

In an attempt to investigate the competition between forcing and eddy damping Finnigan and Ivey (1999, 2000) performed the laboratory simulation suggested in Figure 5.6.2. The 'marginal sea' is really a section of strait channel that lies to the left of an obstacle. The flow there is driven by cooling at the upper surface, which produces vertical convection[1]. The convection does not penetrate completely to the bottom, but does give rise to something like a two-layer exchange flow with most of the sinking occurring at the far left end of the basin (Figure 5.6.3). The two active layers overlie a third, inactive layer. In the area between the sinking and the sill, there is some return flow or recirculation of layer 2 fluid back into layer 1. The lower layer spills over the sill and is hydraulically controlled in all cases.

Since the experimental flow is driven entirely by thermal effects, a thermodynamic balance is needed to replace the statement of conservation of salt. The new constraint may be derived from the density equation, which for a continuously stratified fluid is

$$\frac{\partial \rho}{\partial t *} + \nabla_3^* \cdot (\mathbf{u} * \rho) = \nabla_3^* \cdot (\kappa \nabla_3^* \rho). \qquad (5.6.2)$$

Here κ is a turbulent diffusivity and $\nabla_3^* \cdot$ represents the three-dimensional divergence operator. Relative differences in density throughout the domain are typically small and it has become traditional to work with buoyancy $b = -g \dfrac{\rho - \rho_o}{\rho_o}$ in place of density. Here ρ_o denotes a constant reference density. If the condition of incompressibility $\nabla_3 \cdot \mathbf{u}* = 0$ is used, b may be used in place of ρ in (5.6.2) and the corresponding steady form is

$$\nabla_3 \cdot (\mathbf{u} * b) = \nabla_3 \cdot (\kappa \nabla_3 b).$$

---

[1] The true system is an inverted version of what is shown in Figures 5.1 and 5.2, with the obstacle suspended from the top lid and the left hand basin heated from below.

Integration of this relation over the volume of the marginal sea and use of the divergence theorem gives a relation between the advection of b into the basin at the mouth and the turbulent diffusion of b through the bounding surfaces. The former is given by the integral of v^*b over the entrance of the strait and equals $(Q_1 * b_1 + Q_2 * b_2)$ for a two-layer exchange flow. In the case of pure exchange $(Q_1^* = -Q_2^*)$ the net flux is

$$Q_2^*(b_2 - b_1) = -Q_2^* g(\rho_2 - \rho_1)/\rho_0 = -Q_2^* g'. \tag{5.6.3}$$

The diffusive flux is presumably dominated by fluxes at the air-sea interface $z^* = z_T^*$ and is given in terms of the rates of evaporation E and sensible heat gain H_s by

$$\kappa \frac{\partial b}{\partial z^*}\Bigg|_{z^* = z_T^*} = -B_o = \frac{g}{\rho_o}\left[(H_s - \rho_s L_H E)\frac{\alpha_v}{c_P} - \rho_s E S_s\right] \tag{5.6.4}$$

(e.g. Phillips 1966). The effects of precipitation are ignored. Here S_s is the surface salinity and L_H, α_v and c_P are the latent heat of evaporation, the coefficient of thermal expansion and the specific heat under constant pressure, all of sea water. B_o has units $[L^2/T^3]$ and positive values are associated with a buoyancy loss in the surface waters. If B_o is uniform over the surface area A_s of the basin then the buoyancy budget is given by

$$B_o A_s = g' Q_2^*. \tag{5.6.5}$$

If (5.6.5) is used to replace Q_2^* $(= -Q_1^*)$ in the critical condition (5.5.4), the result may be written.

$$g' = (B_o A_s)^{2/3} w^{*-2/3} D_s^{-1}\left(\frac{1}{d_{1c}^{\,3}} + \frac{1}{(1 - d_{1c})^3}\right)^{1/3}. \tag{5.6.6}$$

This relation is kin to (5.5.8), but now the effect of surface buoyancy flux $B_o A_s$ replaces that of river runoff Q_R^*. Using (5.6.5) this relation can also be written in terms of the lower layer volume flux:

$$Q_2^* = (B_o A_s)^{1/3} w^{*2/3} D_s\left(\frac{1}{d_{1c}^{\,3}} + \frac{1}{(1 - d_{1c})^3}\right)^{-1/3}. \tag{5.6.7}$$

If one were to follow the thread of the previous section, the buoyancy flux would be considered fixed and the value of g' would be minimized (or Q_2^* maximized) over d_{1c} to get a maximal, overmixed state. The overmixed state would be limited by the maximal Q_2^* permitted by the hydraulic constraints for the sill height in question. For a high sill, the maximal Q_2^* occurs when $d_{1c} = .625$ whereas $d_{1c} = 0.5$ for a pure contraction with no sill. The Finnigan and Ivey experiment utilizes a relatively high sill, and thus the former value is appropriate. Substitution d_{1c} into (5.6.7) yeilds

$$(Q_2{}^*)_{\max} = 0.351(B_o A_s)^{1/3} w^{*2/3} D_s . \qquad\qquad (5.6.8)$$

A measure of proximity to this overmixed state for the experimental setup is therefore

$$\left[\frac{Q_2{}^*}{(Q_2{}^*)_{\max}}\right] = 2.849\left(\frac{1}{(d_{1c})^3} + \frac{1}{(1-d_{1c})^3}\right)^{-1/3} . \qquad\qquad (5.6.9)$$

Maximal exchange occurs when $d_{1c}=.625$; submaximal exchange occurs for larger values, or deeper interface levels.

Now consider a sequence of experiments in which the exchange is initially submaximal and the surface buoyancy flux (and therefore $g'Q_2{}^*$) is gradually increased. It is possible, though unlikely, that g' could stay fixed during this process. The increased buoyancy flux would then have to be carried by an elevated $Q_2{}^*$ and, as suggested by (5.6.9), the interface would shallow and the system would evolve towards a maximal state. At the other extreme, $Q_2{}^*$ might remain constant and the extra buoyany flux would be carried by a larger g'. In this situation, the flow would be pushed *away* from the maximal limit: $Q_2{}^*$ would stay the same while $(Q_2{}^*)_{\max}$ would increase. More generally, (5.6.7) suggests that $Q_2{}^*$ must increase more rapidly than $(B_s A_s)^{1/3}$ in order to move towards the maximal state. According to (5.6.6) g' must then increase no more rapidly than $(B_s A_s)^{2/3}$.

Finnigan and Ivey cite four experiments with successively larger B_o (Table 5.1). B_o is lowest for experiment 1 and increases by factors of about 2 or 3 for experiments 2,3 and 4. The value of $Q_2{}^*/(Q_2{}^*)_{\max}$ increases slightly from Experiment 1 to 2, but it decreases for the remaining runs. Although the value of $Q_2{}^*$ increases slightly from 2 to 3 to 4, this trend is compensated for by increases in g'. The experiments therefore indicate that the increase in mixing with B_o does not overcome the increase in g'. There are some practical limits on how hard the experiment can be driven.

The inability of $Q_2{}^*$ to increase sufficiently rapidly to approach a maximal state is attributed to a damping effect associated with the increase in turbulence as the experiment is driven harder. Some evidence of this can be seen in the Figure 5.6.3 photos, in which the thermal forcing increases from top frame to bottom. Another factor is the appearance, with stronger forcing, of a closed circulation cell near the left end of the tank. The two-layer model, in which all surface fluid is converted into lower layer fluid that exits the basin, no longer described the actual situation.

One aspect of this experiment that is unrealistic for applications such as the Mediterranean is the limited extent of the upstream reservoir. Suppose that the local surface buoyancy flux B_o is kept constant and the area A_s of the marginal sea is increased. If the local convection and overturning processes remain unchanged then g' should also remain the same and the increased buoyancy flux $g'Q_2{}^*$ should be contained largely in the flux $Q_2{}^*$. Grimm and Maxworthy (1999) describe an experiment in which A_s is

effectively larger than in the Finnigan and Ivey experiment. [Also, the thermal forcing is replaced by an injection of a brine mixture at the surface.] Both submaximal and maximal (overmixed) exchange flows are observed depending on the strength of the forcing. Nevertheless, it is clear that there is more to overmixing and maximal exchange than perhaps met the eyes of the originators of this idea.

<div align="center">

Table 5.1
(data from the four experiments of Finnigan and Ivey, 2000)

</div>

Experiment	$B_s \times 10^6$ (m^2 s^{-3})	$Q_2*/w*$ (m^2 s^{-1})	g' (m s^{-2})
1	0.4	0.39	0.0036
2	0.9	0.56	0.0029
3	3.0	0.82	0.0068
4	6.0	1.02	0.0080

Exercises

1) (*The Phillips(1969) Red Sea model):* As a simple model of deep convection consider a quarter plane ($z*<0$ and $y*>0$) of initially homogeneous fluid. At the upper boundary $z=0$ the fluid is subjected to a uniform buoyancy flux B_o due to cooling and evaporation. This forcing gives rise to turbulent convection, setting up a hypothetical circulation in which surface fluid approaching the sidewall ($y*=0$) is drawn down. The effects of viscosity are to be ignored and there is no buoyancy flux thorough the sidewall. Present a coherent argument, purely on dimensional grounds, that

$$v* \propto (B_o y*)^{1/3} f(z*/y*),$$

where v represents the time-mean y-velocity of the statistically steady flow that eventually occurs. Also, f is an unknown universal function.

Next suppose that the inflow and outflow must cross a sill of depth D_s that lies a distance L from the vertical wall. A plausible generalization of the above relation is then

$$v* \propto (B_o y*)^{1/3} f(z*/y*)g(z*/D_s).$$

If the flow is now imagined to occur in a channel of width $w*$, compute the exchange transport and comment on any similarities with (5.5.12).

Figure Captions

Figure 5.6.1 Bathymetry of the Strait of Gibraltar.

Figure 5.6.2 Sketches of the flow forcing and resulting two-layer regime in the experiments of Finnigan and Ivey (2000). The lowest layer is relatively inactive.

Figure 5.6.3 Photographs of three realizations of the Finnigan and Ivey (2000) experiment with progressively larger surface buoyancy flux (applied where the surface is marked by a thickened line). From top to bottom, the frames correspond to Experiments 2, 3, and 4 in Table 1.
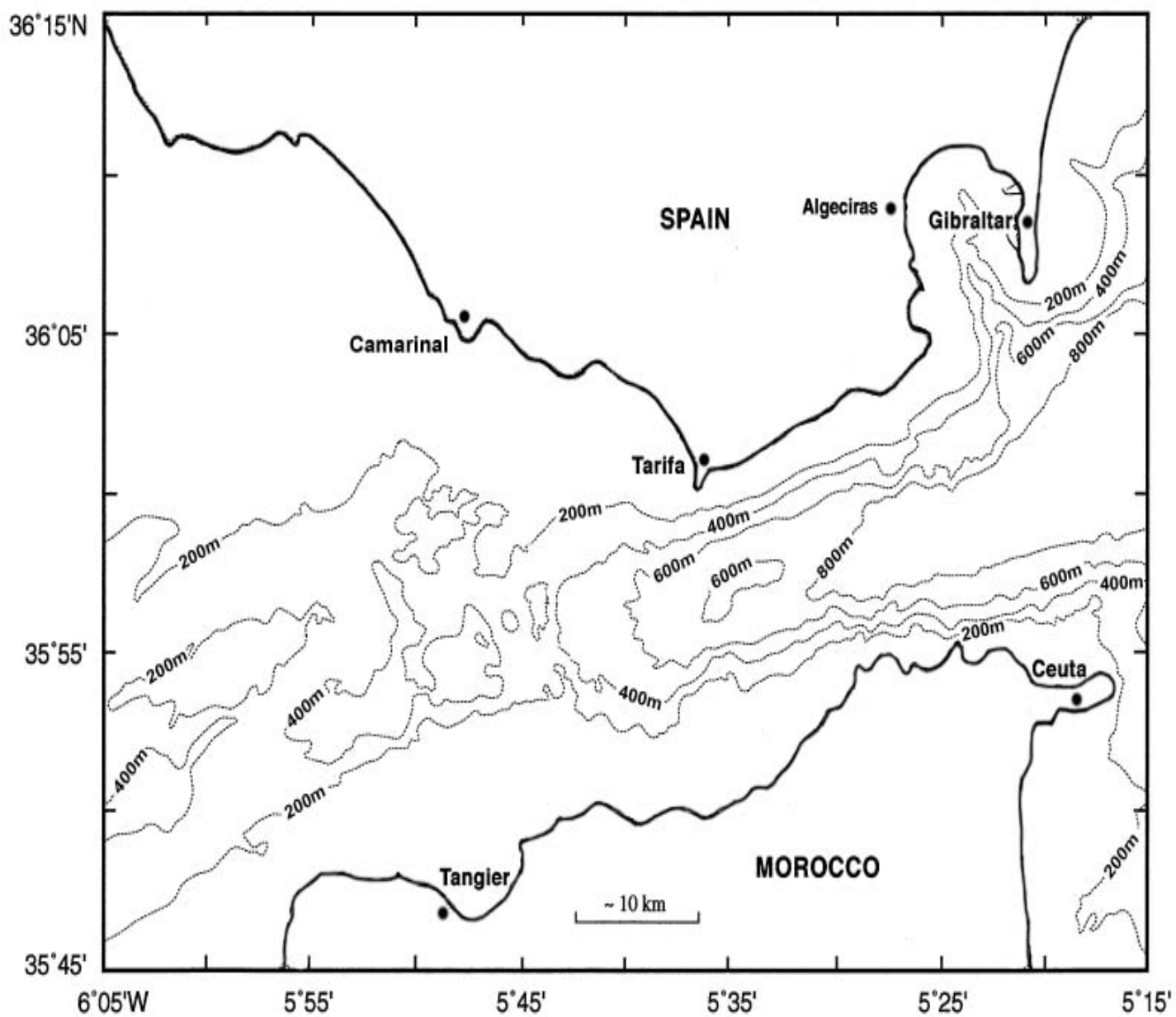
Figure 5.6.1

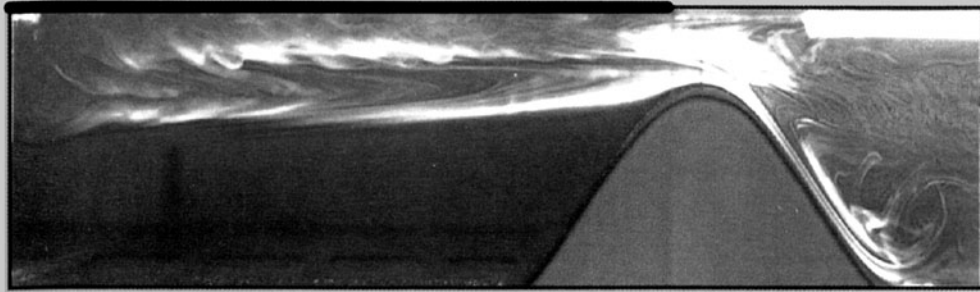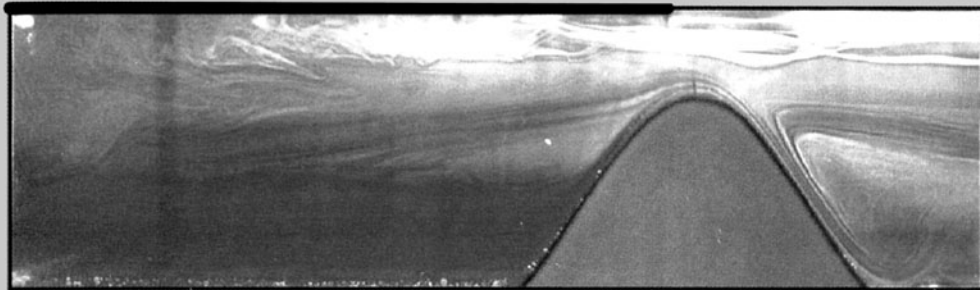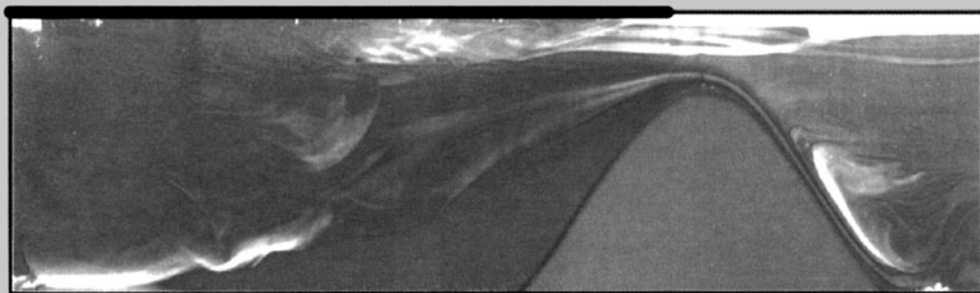B_o

layer 1

layer 2

inactive layer
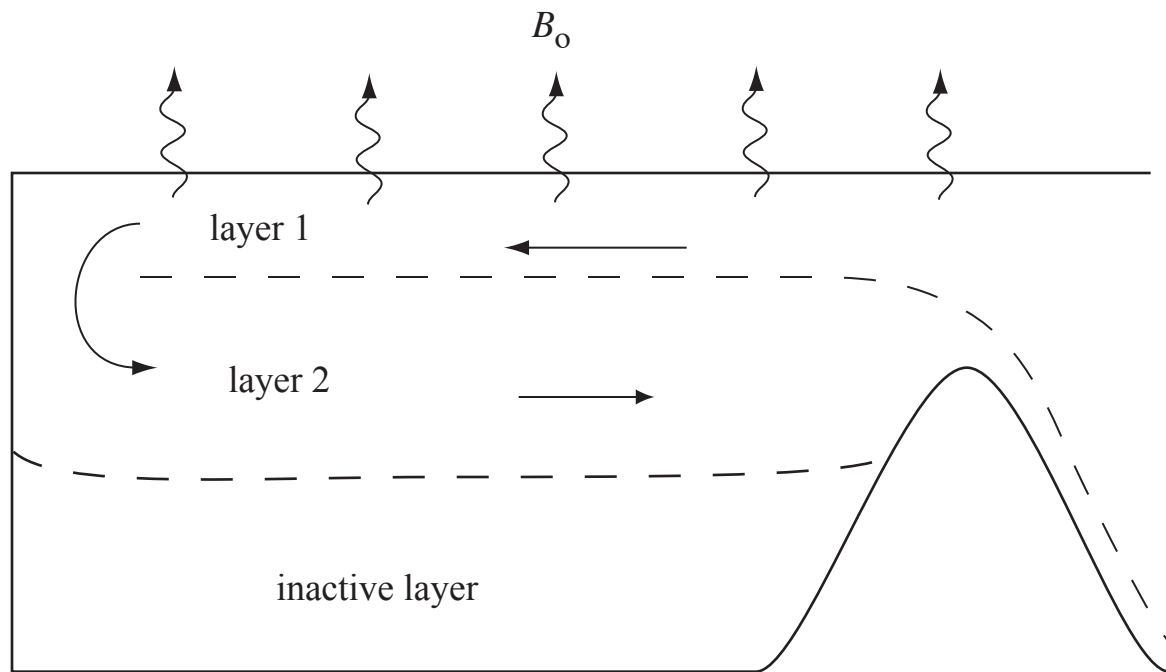
Figure 5.6.2

(a)

(b)

(c)

Low resolution version of Figure 5.6.3